10th World Congress on Structural and Multidisciplinary Optimization
May 19 -24, 2013, Orlando, Florida, USA

Free-form Optimization Method for Designing Spatial Frame Structure

M. Shimoda[1], Y. Liu[2] and F. Hayashi[3]

[1] Toyota Technological Institute,Nagoya, Japan, shimoda@toyota-ti.ac.jp
[2] Toyota Technological Institute,Nagoya, Japan, liuyang@toyota-ti.ac.jp
[3] Aishin AW Co., Ltd., Anjo City, Japan,

1. Abstract
In this paper, we propose a parameter-free shape optimization method for designing the smooth optimal free-form of a 3D frame structure. A stiffness design problem where the compliance is minimized under a volume constraint is solved as an example of shape design problems of frame structures. The optimum design problem is formulated as a distributed-parameter shape optimization problem under the assumptions that each member is varied in the out-of-plane direction to the neutral axis and that the cross section is prismatic. The shape gradient function and the optimality conditions for this problem are then theoretically derived. The optimal curvature distribution is determined by applying the derived shape gradient function to each member as a pseudo distributed force to vary the frame, while minimizing the objective functional. We call this method the free-form optimization method for frames, i.e., a gradient method in a Hilbert space. The validity and practical utility of this method were verified through several design examples. It was confirmed that axial-force-carrying structures were obtained by this method.
2. Keywords: Optimum design; Shape optimization; Structural optimization; Frame structure; Free form.

3. Introduction
Frame structures composed of straight or curved members may be regarded as eco-friendly structures. Although the members are slender, the assembled structure has high load-carrying capacity and can contribute to a lighter weight and resource savings. Such structures are extensively used in various fields of engineering, especially in space, civil and architectural structures. Their lightness and slenderness are apt to result in a lack of stiffness or strength. Therefore, in the design of a frame structure, it is important to optimize its shape in order to satisfy the requirements of various structural characteristics, while achieving a lighter weight.
In previous studies, most of the methods proposed for the shape optimization of frame structures are parametric approaches, which require shape parameterization in advance. For example, Hashemian *et al.* applied a genetic algorithm (GA) method to optimize the geometric parameters of a squared lattice cylindrical shell under a compressive axial load in order to achieve the maximum buckling load [1]. Winslow *et al.* reported a design tool for synthesis of optimal grid structures, using a multi-objective GA to vary rod directions over the surface in response to two or more load cases [2]. Rial used simulated annealing (SA) to find the optimum parameters of one-layer lattice shells that have more effect on reducing cost in a way comparable to plane structures [3]. Jarraya *et al.* developed a sequential quadratic programming (SQP) method to minimize the von Mises stress of beam structures parameterized by Bezier and B-spline curves [4]. Ohsaki *et al.* applied the SQP method to multi-objective shape optimization of latticed shells parameterized by a Bezier surface [5]. These methods are effective in reducing the number of design variables. However, the parameterization process requires knowledge and experience, and selecting the right parameter for complicated forms is troublesome for designers. Moreover, the shapes obtained by parametric methods are strongly influenced by the defined parameters.
In contrast, fewer non-parametric methods have been proposed than parametric methods. For example, Chen *et al.* proposed a Generalised Reduced Gradient (GRG) method for finding the optimum shape of a lattice space frame with the maximum buckling load [6]. Ohmori *et al.* applied a nonlinear programming technique to obtain a bend-free surface of space structures [7]. Kuijvenhoven *et al.* introduced a particle-spring method for finding the optimal form of grid shells consisting of flexible members [8]. These methods are formulated in the discrete, or the matrix-based system. Therefore, they are suitable for design problems with a limited number of nodes. As the shapes obtained are strongly influenced by discretization, they are not well-suited for design problems of arbitrary free-form frame structures.
In this paper, we present a new parameter-free shape optimization method for the optimal free-form design of three-dimensional frame structures. This method is formulated in the continuous system and determines the optimal free-form without any advance shape parameterization. All nodes can be treated as design variables. Therefore, the shape obtained is not influenced by discretization and parameterization.
In the following sections, the governing equation of the frame structure, the formulation of the problem, and the free-form optimization method will be described. Then, numerical analysis results for two design problems will be

presented to demonstrate the effectiveness and practical utility of our solution.

4. Shape optimization problem of frame structure

4.1. Governing equation of frame structure

As shown in Fig. 1, Timoshenko beams $\{\Omega^j\}_{j=1,2,\ldots,N}$ compose a frame structure which can be represented by a bounded domain $\Omega = \bigcup_{j=0}^{N} \Omega^j \subset \mathbb{R}^3$, where N is the number of beams. The notations (x_1, x_2, x_3) and (X_1, X_2, X_3) in the figure indicate the local coordinate system and the global coordinate system, respectively.

$$\Omega^j = \left\{ \left(x_1^j, x_2^j, x_3^j\right) \in \mathbb{R}^3 \,\middle|\, \left(x_1^j, x_2^j\right) \in A^j \subset \mathbb{R}^2, x_3^j \in S^j \subset \mathbb{R} \right\}, \quad \Gamma^j = \partial A^j \times S^j, \quad \Omega^j = A^j \times S^j, \tag{1}$$

where S^j, A^j, Ω^j express the neutral axis, cross section and circumference surface of beam j, respectively. It is assumed that the material is isotropic and homogeneous. The weak form equation in terms of $(\boldsymbol{w}, \boldsymbol{\theta})$ can be expressed as Equation (2).

$$a\left((\boldsymbol{w}, \boldsymbol{\theta}), (\bar{\boldsymbol{w}}, \bar{\boldsymbol{\theta}})\right) = l\left((\bar{\boldsymbol{w}}, \bar{\boldsymbol{\theta}})\right), \quad \forall (\bar{\boldsymbol{w}}, \bar{\boldsymbol{\theta}}) \in U, \quad (\boldsymbol{w}, \boldsymbol{\theta}) \in U, \tag{2}$$

where $\boldsymbol{w} = \{w_i\}_{i=1,2,3}$ expresses a displacement vector in the x_1, x_2, x_3 directions of the local coordinate system, and $\boldsymbol{\theta} = \{\theta_i\}_{i=1,2,3}$ expresses a rotation vector around the x_1, x_2, x_3 axes. $(\bar{\ })$ expresses a variation, and U expresses admissible space in which the given constraint conditions of $(\boldsymbol{w}, \boldsymbol{\theta})$ are satisfied. In addition, the bilinear form $a(\cdot,\cdot)$ and the linear form $l(\cdot)$ are defined respectively as shown below.

$$\begin{aligned} a\left((\boldsymbol{w}, \boldsymbol{\theta}), (\bar{\boldsymbol{w}}, \bar{\boldsymbol{\theta}})\right) = \sum_{j=1}^{N} \int_{\Omega^j} \Big\{ & \left(w_{1,3} - x_2\theta_{3,3} - \theta_2\right) \mu \left(\bar{w}_{1,3} - x_2\bar{\theta}_{3,3} - \bar{\theta}_2\right) \\ & + \left(w_{2,3} + x_1\theta_{3,3} + \theta_1\right) \mu \left(\bar{w}_{2,3} + x_1\bar{\theta}_{3,3} + \bar{\theta}_1\right) \\ & + \left(w_{3,3} - x_1\theta_{2,3} + x_2\theta_{1,3}\right) E \left(\bar{w}_{3,3} - x_1\bar{\theta}_{2,3} + x_2\bar{\theta}_{1,3}\right) d\Omega, \end{aligned} \tag{3}$$

$$l\left((\boldsymbol{w}, \boldsymbol{\theta})\right) = \sum_{j=1}^{N} \int_{S^j} \left(F_i \bar{w}_i + C_1\bar{\theta}_1 - C_2\bar{\theta}_2 + C_3\bar{\theta}_3\right) dS + Q_i \bar{w}_i \Big|_{A_\alpha}^{j} + M_i \bar{\theta}_i \Big|_{A_\alpha}^{j}, \tag{4}$$

where $\boldsymbol{F} = \{F_i\}_{i=1,2,3}$ and $\boldsymbol{C} = \{C_i\}_{i=1,2,3}$ are the force and couple vectors per unit length applied to beam S, $\boldsymbol{Q} = \{Q_i\}_{i=1,2,3}$ and $\boldsymbol{M} = \{M_i\}_{i=1,2,3}$ are the shearing force and bending moment vectors applied to the boundaries $\boldsymbol{A}_\alpha (\alpha = 1, 2)$. The notation μ is the Lame constant, and E is the Young's modulus. Moreover, the tensor subscript notation uses Einstein's summation convention and a partial differential notation for the spatial coordinates $(\cdot)_{,i} = \partial(\cdot)/\partial x_i$.

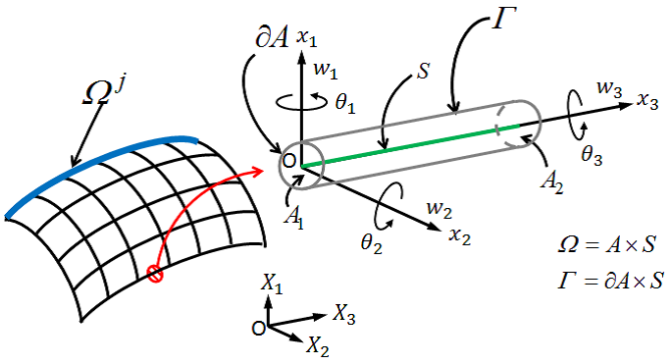

Figure 1: Frame structure composed of Timoshenko beams

4.2. Domain variation

In the frame structure as shown in Fig. 2, consider that a beam j having an initial domain Ω^j, neutral axis S^j, and boundary $A_\alpha^j (\alpha = 1, 2)$ undergoes out-of-plane domain variation $\boldsymbol{V}^j$ (design velocity field) in the normal direction to the neutral axis such that its domain, mid-area, boundary and side surface become Ω_s^j, S_s^j and $A_{\alpha_s}^j$, respectively. The subscript s expresses the iteration history of the domain variation. Defining the notation $\boldsymbol{n}_1$ and $\boldsymbol{n}_2$ as outward unit normal vectors of the neutral axis in the $\boldsymbol{x}_1$ and $\boldsymbol{x}_2$ directions, $\boldsymbol{V}^j$ can be expressed by

$$\boldsymbol{V}^j = \left(\boldsymbol{V}^j \cdot \boldsymbol{n}_1^j\right)\boldsymbol{n}_1^j + \left(\boldsymbol{V}^j \cdot \boldsymbol{n}_2^j\right)\boldsymbol{n}_2^j . \tag{5}$$

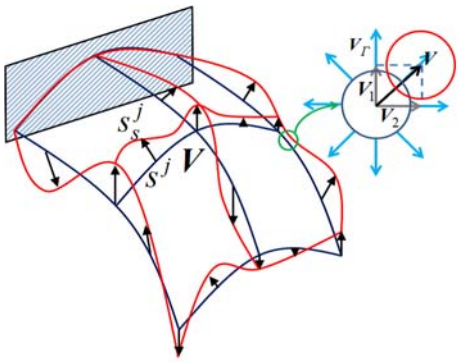

Figure 2: Shape variation of frame structure

4.3. Compliance minimization problem

Let us consider a free-form optimization problem for maximizing the stiffness of a frame structure. Letting the state equation in Eq. (2) be the constraint condition and the compliance the objective functional to be minimized, a distributed-parameter shape optimization problem for finding the optimal design velocity field $\boldsymbol{V}^j$ can be formulated as shown below:

$$\begin{aligned} &\text{Given} && \Omega, && (6)\\ &\text{find} && \boldsymbol{V} \text{ or } \Omega_s, && (7)\\ &\text{that minimizes} && l((\boldsymbol{w},\boldsymbol{\theta})), && (8)\\ &\text{subject to} && \text{Equation (2) and } M\left(=\sum_{j=1}^{N}\int_{S^j} A^j dS\right) \le \hat{M}, && (9) \end{aligned}$$

where M and $\hat{M}$ denote the volume and its constraint value, respectively.

Letting $(\bar{\boldsymbol{w}},\bar{\boldsymbol{\theta}})$ and Λ denote the Lagrange multipliers for the state equation and volume constraints, respectively, the Lagrange functional L associated with this problem can be expressed as

$$L\left(\Omega,(\boldsymbol{w},\boldsymbol{\theta}),(\bar{\boldsymbol{w}},\bar{\boldsymbol{\theta}}),\Lambda\right) = l\left((\boldsymbol{w},\boldsymbol{\theta})\right) + l\left((\bar{\boldsymbol{w}},\bar{\boldsymbol{\theta}})\right) - a\left((\boldsymbol{w},\boldsymbol{\theta}),(\bar{\boldsymbol{w}},\bar{\boldsymbol{\theta}})\right) + \Lambda\left(M-\hat{M}\right). \tag{10}$$

The material derivative $\dot{L}$ of the Lagrange functional can be derived as shown in Eq. (12) below using the velocity field $\boldsymbol{V}$ and an outward unit normal vector $\boldsymbol{n}$ on the virtual cross section.

$$\dot{L} = l((\bar{\boldsymbol{w}}',\bar{\boldsymbol{\theta}}')) + l((\boldsymbol{w}',\boldsymbol{\theta}')) - a((\boldsymbol{w}',\boldsymbol{\theta}'),(\bar{\boldsymbol{w}},\bar{\boldsymbol{\theta}})) - a((\boldsymbol{w},\boldsymbol{\theta}),(\bar{\boldsymbol{w}}',\bar{\boldsymbol{\theta}}'))\boldsymbol{n} + \dot{\Lambda}\left(M-\hat{M}\right) + \sum_{j=1}^{N}\left\langle G^j\boldsymbol{n},\boldsymbol{V}\right\rangle,\ \boldsymbol{V}\in C_\Theta, \tag{11}$$

$$\begin{aligned} \left\langle G^j\boldsymbol{n},\boldsymbol{V}\right\rangle \equiv\ & \int_{\Gamma^j} G^j\boldsymbol{V}_\Gamma\cdot\boldsymbol{n}\ d\Gamma + \int_{S^j} G_0\boldsymbol{V}\cdot\boldsymbol{n}\ dS\\ =& -\int_{\Gamma^j}\Big\{\left(w_{1,3}-x_2\theta_{3,3}-\theta_2\right)\mu\left(\bar{w}_{1,3}-x_2\bar{\theta}_{3,3}-\bar{\theta}_2\right)+\left(w_{2,3}+x_1\theta_{3,3}+\theta_1\right)\mu\left(\bar{w}_{2,3}+x_1\bar{\theta}_{3,3}+\bar{\theta}_1\right)\\ &+\left(w_{3,3}-x_1\theta_{2,3}+x_2\theta_{1,3}\right)E\left(\bar{w}_{3,3}-x_1\bar{\theta}_{2,3}+x_2\bar{\theta}_{1,3}\right)\Big\}\boldsymbol{V}_\Gamma\boldsymbol{n}\ d\Gamma\\ &+\int_{S^j}\Big\{\Lambda AH+\Big[\Big\{F_i\left(w_i+\bar{w}_i\right)+C_1\left(\theta_1+\bar{\theta}_1\right)-C_2\left(\theta_2+\bar{\theta}_2\right)+C_3\left(\theta_3+\bar{\theta}_3\right)\Big\},_j n_j\\ &+\Big\{F_i\left(w_i+\bar{w}_i\right)+C_1\left(\theta_1+\bar{\theta}_1\right)-C_2\left(\theta_2+\bar{\theta}_2\right)+C_3\left(\theta_3+\bar{\theta}_3\right)\Big\}H\Big]\Big\}\boldsymbol{V}\boldsymbol{n}dS, \end{aligned} \tag{12}$$

where $\boldsymbol{G}^j$ expresses the shape gradient function, which is a coefficient function in terms of $\boldsymbol{V}_\Gamma\boldsymbol{n}$ or $\boldsymbol{V}\boldsymbol{n}$, and the notation H denotes the curvature of the neutral axis. The notations $(\cdot)'$ and $(\dot{\cdot})$ are the shape derivative and the material derivative with respect to the domain variation, respectively [9].

The optimality conditions of the Lagrangian function L with respect to $(\boldsymbol{w},\boldsymbol{\theta})$, $(\bar{\boldsymbol{w}},\bar{\boldsymbol{\theta}})$ and Λ are expressed as shown below.

$$a\left((\boldsymbol{w},\boldsymbol{\theta}),(\bar{\boldsymbol{w}}',\bar{\boldsymbol{\theta}}')\right) = l\left((\bar{\boldsymbol{w}}',\bar{\boldsymbol{\theta}}')\right),\quad \forall(\bar{\boldsymbol{w}}',\bar{\boldsymbol{\theta}}')\in U, \tag{13}$$

$$a\left(\left(\boldsymbol{w}',\boldsymbol{\theta}'\right),\left(\bar{\boldsymbol{w}},\bar{\boldsymbol{\theta}}\right)\right)=l\left(\left(\boldsymbol{w}',\boldsymbol{\theta}'\right)\right),\quad \forall\left(\boldsymbol{w}',\boldsymbol{\theta}'\right)\in U, \tag{14}$$

$$\dot{\Lambda}\left(M-\hat{M}\right)=0,\quad M-\hat{M}\le 0,\quad \Lambda\ge 0. \tag{15) (16) (17}$$

When the optimality conditions are satisfied, $\dot{L}$ becomes

$$\dot{L}=\sum_{j=1}^{N}\left\langle G^j\boldsymbol{n},\boldsymbol{V}\right\rangle. \tag{18}$$

Consider a beam of uniform rectangular section with height $\boldsymbol{h}_1$ and width $\boldsymbol{h}_2$ as shown in Fig. 3. The relationship of $\left(\boldsymbol{V}\cdot\boldsymbol{n}^t\right)\boldsymbol{n}^t=\left(-\boldsymbol{V}\cdot\boldsymbol{n}^b\right)\boldsymbol{n}^b$, $\left(\boldsymbol{V}\cdot\boldsymbol{n}^r\right)\boldsymbol{n}^r=\left(-\boldsymbol{V}\cdot\boldsymbol{n}^l\right)\boldsymbol{n}^l$ is assumed by using the notations $\boldsymbol{n}^t$, $\boldsymbol{n}^b$, $\boldsymbol{n}^r$ and $\boldsymbol{n}^l$, which denote a unit outward normal vector at the top, bottom, left and right surface of the cross section, respectively. Moreover, let $\boldsymbol{n}_1$, $\boldsymbol{n}_2$ denote unit vectors from the neutral axis in the directions of axis $\boldsymbol{x}_1$ and $\boldsymbol{x}_2$, and then they have the relationship of $\boldsymbol{n}_1=\boldsymbol{n}^t=-\boldsymbol{n}^b$, $\boldsymbol{n}_2=\boldsymbol{n}^r=-\boldsymbol{n}^l$, respectively.

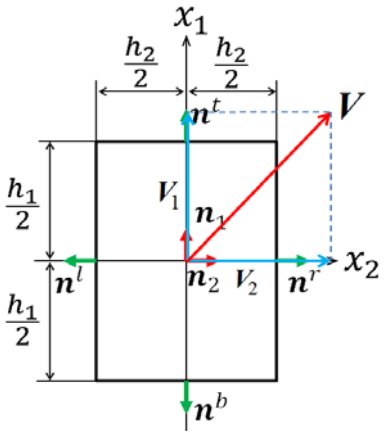

Figure 3: Sign notation of cross section

The shape gradient functions G_1^j, G_2^j, G_0^j (i.e., sensitivity functions) for this problem are derived as the following equations by considering the self-adjoint relationship $\left(\left(\boldsymbol{w},\boldsymbol{\theta}\right)=\left(\bar{\boldsymbol{w}},\bar{\boldsymbol{\theta}}\right)\right)$, which are obtained from Eq. (13) and Eq. (14).

$$\left\langle G^j\boldsymbol{n},\boldsymbol{V}\right\rangle=\int_{S^j}\left(G_1^j\boldsymbol{V}\cdot\boldsymbol{n}_1+G_2^j\boldsymbol{V}\cdot\boldsymbol{n}_2+G_0^j\boldsymbol{V}\cdot\boldsymbol{n}\right)dS, \tag{19}$$

$$G_1^j=2h_1h_2\left\{Ew_{3,3}\theta_{2,3}-\mu\theta_{3,3}\left(w_{2,3}+\theta_1\right)\right\}, \tag{20}$$

$$G_2^j=2h_1h_2\left\{\mu\theta_{3,3}\left(w_{1,3}-\theta_2\right)-Ew_{3,3}\theta_{1,3}\right\}, \tag{21}$$

$$G_0^j=AH+\left\{2\left(F_iw_i+C_1\theta_1-C_2\theta_2+C_3\theta_3\right)H\right\}. \tag{22}$$

5. Free-form optimization method for frame structure

The free-form optimization method described here was initially proposed by Shimoda for solving the shape optimization problem of shell structures [10, 11]. The method is based on the H^1 gradient method in a Hilbert space [12, 13, 14]. It is a node-based shape optimization method that can treat all nodes as design variables and does not require any design variable parameterization. In this study, we apply this method to obtain a free-form shape optimization method for frame structures.

With this method the negative shape gradient function $-\boldsymbol{G}\left(\boldsymbol{X}\right)$ is applied as a distributed force to a pseudo-elastic frame structure in the normal direction to the neutral axis under a Robin boundary condition, i.e., an elastic support condition with a distributed spring constant $\alpha>0$, and shape design constraint conditions as shown in Fig. 4. The shape gradient function is not applied directly to the shape variation but rather is replaced by a force. This makes it possible both to reduce the objective functional and to maintain smoothness, i.e., mesh regularity, which is the most distinctive feature of this method. The shape variation $\boldsymbol{V}$ is determined in the pseudo-elastic frame analysis, which is called velocity analysis, and the obtained $\boldsymbol{V}$ is used to update the shape. The governing equation of the velocity analysis for $\boldsymbol{V}=\left(V_1,V_2,V_3\right)$ is expressed as Eq. (23).

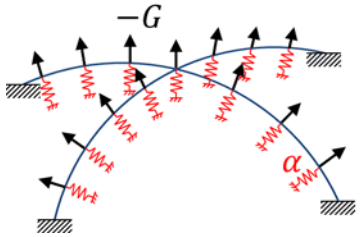

Figure 4: Schematic of free-form optimization method for frames

$$a\left((\boldsymbol{V},\boldsymbol{\theta}),\left(\bar{\boldsymbol{w}},\bar{\boldsymbol{\theta}}\right)\right)+\alpha\left\langle(\boldsymbol{V}\cdot\boldsymbol{n})\boldsymbol{n},\left(\bar{\boldsymbol{w}},\bar{\boldsymbol{\theta}}\right)\right\rangle=-\left\langle G\boldsymbol{n},\left(\bar{\boldsymbol{w}},\bar{\boldsymbol{\theta}}\right)\right\rangle,\ \forall\left(\bar{\boldsymbol{w}},\bar{\boldsymbol{\theta}}\right)\in C_{\Theta},\ (\boldsymbol{V},\boldsymbol{\theta})\in C_{\Theta}, \tag{23}$$

$$C_{\Theta}=\left\{(V_1,V_2,V_3,\theta_1,\theta_2,\theta_3)\in\left(H^1(S)\right)^6\ \middle|\ \text{satisfy Dirichlet condition for shape variation}\right\}. \tag{24}$$

It has been confirmed that this gradient method reduces the Lagrange functional L as follows. When the state equation and the adjoint equation are satisfied, the perturbation expansion of the Lagrange functional L can be written as

$$\Delta L=\sum_{j=1}^{N}\left\langle G\boldsymbol{n},\Delta s(\boldsymbol{V},\boldsymbol{\theta})\right\rangle+O(|\Delta s|^2), \tag{25}$$

Substituting Eq. (23) into Eq. (25) and taking into account the positive definitiveness of the elastic tensors, the following relationship is obtained when Δs is sufficiently small:

$$\Delta L=-\sum_{j=1}^{N}\left\{a(\Delta s(\boldsymbol{V},\boldsymbol{\theta}),\Delta s(\boldsymbol{V},\boldsymbol{\theta}))+\alpha\left\langle(\Delta s\boldsymbol{V}\cdot\boldsymbol{n})\boldsymbol{n},\Delta s(\boldsymbol{V},\boldsymbol{\theta})\right\rangle\right\}<0. \tag{26}$$

In problems where convexity is assured, this relationship definitely reduces the Lagrange functional in the process of updating the frame shape using the design velocity field $\boldsymbol{V}$ determined by Eq. (23).
The optimal free-form frame structure is obtained by repeating a process consisting of (1) stiffness analysis, (2) sensitivity analysis for calculating the shape gradient functions, (3) velocity analysis and (4) shape updating. The analyses in (1) and (3) are conducted using a standard general-purpose FEM code.

6. Results Calculated with the Free-form Optimization Method

The proposed method was applied to two design problems to verify its validity and practical utility. In each design problem, the beams had a uniformly square cross-section of width W=20 (mm) and a volume constraint was set as 105% of the initial shape.

6.1. Square lattice model

The first problem considered is a square lattice model (size: 1000 (mm)×1000 (mm)) subject to torsion as shown in Fig. 5. The boundary conditions of the stiffness analysis and the velocity analysis are shown in Fig. 5(a) and (b), respectively. Moreover, the model was meshed using one-dimensional elements, and each beam between two joint points was divided to multiple the number of elements as shown in Fig. 5(a). The notation SPC in Fig. 5(a) expresses the single point constraint, and 1, 2, and 3 express the x, y, z translational degrees of freedom, respectively. Figure 6 shows the optimal shape obtained. It is obvious that an X-shaped bead was created. Figure

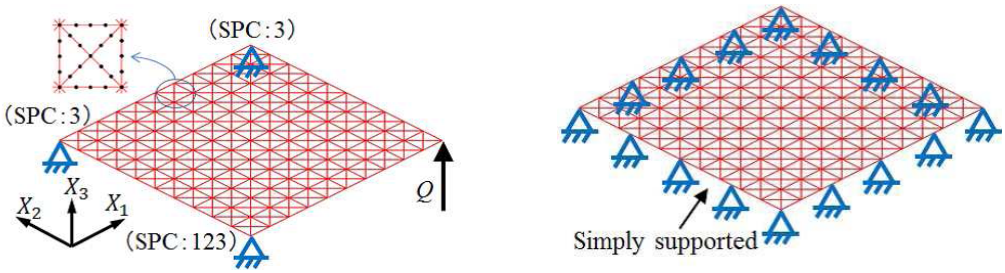

(a) Stiffness analysis (b) Velocity analysis

Figure 5: Boundary conditions of square lattice model

7(a) shows the iteration convergence histories of the compliance and the volume, where the values were normalized to those of the initial shape. The compliance of the obtained shape was much reduced and became 0.09 times that of the initial shape, while satisfying the given volume constraint. A comparison of the ratio of strain energy between the initial shape and the optimal shape is shown in Fig. 7(b), where the values are normalized to the total strain energy of the initial shape. The obtained structures became axial-force-carrying.

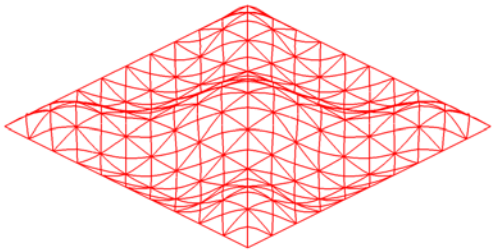

Figure 6: Obtained shape of square lattice

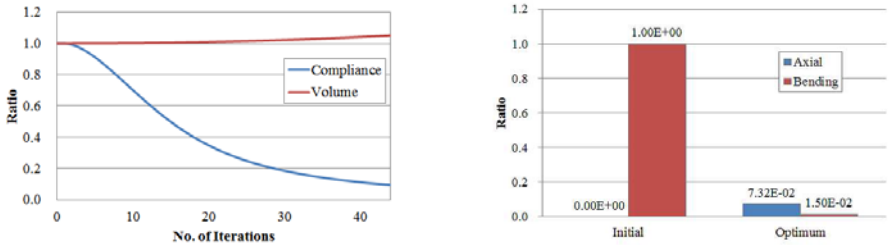

(a) Iteration histories (b) Component ratio of strain energy

Figure 7: Optimization results of square lattice model

6.2. U-shaped lattice

The second problem concerns a U-shaped lattice (1000 (mm)×1200 (mm)×400 (mm)). The boundary conditions of the stiffness analysis and the velocity analysis are shown in Fig. 8(a) and (b). In the stiffness analysis, one edge was fixed completely and equilibrium forces were applied in the inward direction to the other edge. In the velocity analysis, all boundaries were pin supported. The obtained shape is shown in Fig. 9(a), where the shape is greatly curved at the middle of the bend section. Figure 9(b) shows a comparison of the strain energy components between the initial and optimal shapes. The strain energy of the initial shape was approximately 100% dominated by the bending component, but that of the optimal shape was almost entirely dominated by the axial component as expected. Compliance was reduced by approximately 94% while satisfying the volume constraint.

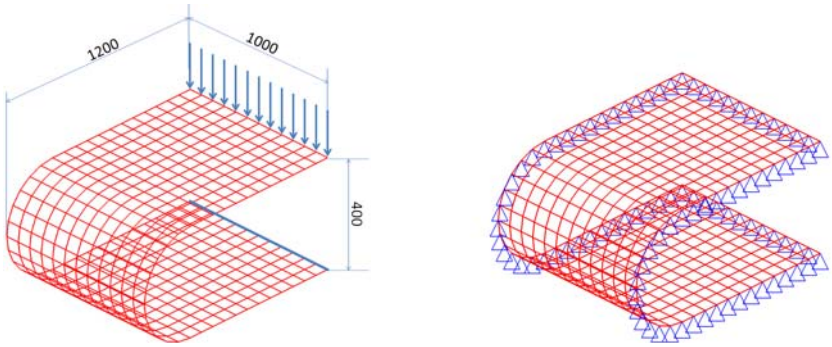

(a) Stiffness analysis (b) Velocity analysis

Figure 8: Boundary conditions of U-shaped lattice

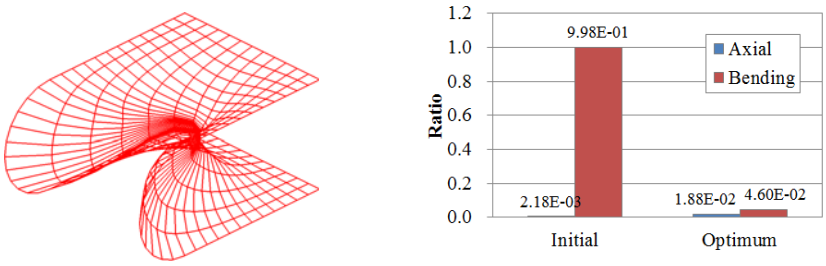

(a) Obtained shape (b) Component ratio of strain energy

Figure 9: Optimization results of U-shaped lattice

7. Conclusions

A new free-form optimization method was presented for designing the optimal shape of frame structures. With the aim of maximizing the stiffness, a compliance minimization problem subject to a volume constraint was formulated as a non-parametric shape optimization problem under the assumptions that the frame was varied in the out-of-plane direction to the neutral axis and the cross section was prismatic. With this method, (1) the optimal smooth curvature distribution of a frame structure can be determined without any shape parameterization; (2) it is able to deal with large-scale shape optimization problems; (3) a smooth and natural frame shape can be obtained. The validity and practical utility of the proposed method were verified through two design examples. The results confirmed that the frame structures obtained were changed from the initial bending-carrying structures to axial-force-carrying ones.

8. References

[1] AH. Hashemian, MH. Kargarnovin and JE. Jam, Optimization of geometric parameters of latticed structures using genetic algorithm, *Aircraft Engineering and Aerospace Technology*, 83, 59–68, 2011.

[2] P. Winslow, S. Pellegrino and S. Sharma, Multi-objective optimization of free-form grid structures, *Structural and Multidisciplinary Optimization* , 40, 257–269, 2010.

[3] B. O. Rial, Shape optimization of one layer lattice shells using simulated annealing, *EngOpt 2008 - International Conference on Engineering Optimization*, 2008.

[4] A. Jarraya, F. Dammak, S. Abid and M. Haddar, Shape and thickness optimization performance of a beam structure by sequential quadratic programming method. *Journal of Failure Analysis and Prevention*, 7, 50–55, 2007.

[5] M. Ohsaki and S. Fujita, Multiobjective shape optimization of latticed shells for elastic stiffness and uniform member lengths. *Proceedings of International Symposium on Algorithmic Design for Architecture and Urban Design 2011*, Tokyo, 2011.

[6] Pei-Shan Chen and M. Kawaguchi, Optimization for Maximum Buckling Load of a Lattice Space Frame with Nonlinear Sensitivity Analysis, *International Journal of Space Structures*, 21 (2), 111-118, 2006.

[7] H. Ohmori and K. Yamamoto, Shape Optimization of Shell and Spatial Structures for Specified Stress Distribution (Part2: Space Frame Analysis), *Journal of IASS*, 39 (3), 147-157, 1998.

[8] M. Kuijvenhoven and P. Hoogenboom, Particle-spring method for form finding grid shell structures consisting of flexible members. *Journal of the International Association for Shell and Spatial Structures*, 53, 31–38, 2012.

[9] K. K. Choi and N. H. Kim, *Structural Sensitivity Analysis and Optimization*, 1, Springer, New York, 2005.

[10] M. Shimoda, Y. Liu and M. Yonekura, Multi-objective free-form optimization of shell structures. *Proceedings of 53rd AIAA/ASME/ASCE/AHS/ASC Structures, Structural Dynamics and Materials Conference*, AIAA, 2012.

[11] M. Shimoda, Free-form optimization method for designing automotive shell structures. *SAE, International Journal of Passenger Cars- Electronic and Electrical Systems*, 4, 42–54, 2011.

[12] H. Azegami, A Solution to Domain Optimization Problems, *Transactions of Japan Society of Mechanical Engineerings*, Series A, No. 60, pp. 1479-1486, 1994 (in Japanese).

[13] M. Shimoda, H. Azegami and T. Sakurai, Traction Method Approach to Optimal Shape Design Problems, *SAE Transactions, Journal of Passenger Cars*, Section 6, Vol. 106, pp. 2355-2365, 1998.

[14] H. Azegami, K. Takeuchi, A smoothing method for shape optimization: Traction method using the Robin condition. *International Journal of Computational Methods*, 3, 21–33, 2006.